Spectral and spatial distribution of polarization at the $LaAlO_3/SrTiO_3$ interface

A. Rubano and M. Fiebig
Helmholtz-Institut für Strahlen- und Kernphysik, Universität Bonn, Nussallee 14-16, DE-53115 Bonn, Germany

D. Paparo,* A. Marino, D. Maccariello, U. Scotti di Uccio, F. Miletto Granozio, and L. Marrucci
CNR-SPIN and Dipartimento di Scienze Fisiche, Università di Napoli "Federico II," Complesso Universitario di Monte Sant'Angelo, via Cintia, IT-80126 Napoli, Italy

C. Richter, S. Paetel, and J. Mannhart
Center for Electronic Correlations and Magnetism, University of Augsburg, DE-86135 Augsburg, Germany
(Received 13 August 2010; revised manuscript received 3 February 2011; published 5 April 2011; publisher error corrected 7 April 2011)

The polarization induced at the $LaAlO_3/SrTiO_3$ interface has been explored by optical second harmonic generation (SHG) spectroscopy. Our data reveal that an orbital reconstruction of the $SrTiO_3$ surface occurs when three epitaxial monolayers of $LaAlO_3$ are deposited on top of it. The reconstruction manifests as a spectral modification of a $Ti^{4+}(3d)$ state at the $LaAlO_3/SrTiO_3$ interface which is accompanied by a displacement of the Ti^{4+} ions in adjacent $SrTiO_3$ monolayers in order to compensate for the polarization discontinuity induced at the interface. According to the SHG experiment, the carriers transferred to the interface are trapped because in spite of the orbital reconstruction, the interface remains insulating. The onset of conductivity with the formation of a two-dimensional electron liquid appears to be a subordinate effect related to a minority of carriers and occurs upon further increase of the $LaAlO_3$ coverage.

DOI: 10.1103/PhysRevB.83.155405 PACS number(s): 73.20.−r, 73.40.−c, 77.22.Ej, 42.65.Ky

I. INTRODUCTION

The technology for the growth of ultrathin oxide films or heterostructures is approaching the level of atomic control achieved with semiconductors.[1] Yet, in contrast to semiconductors, strong electron correlations and the large polarizability of the oxygen ions lead to novel and sometimes exotic states at the interface. One of the most prominent examples is the formation of a two-dimensional electron liquid (2DEL) at the interface between two textbook-type band insulators, $LaAlO_3$ (LAO) and $SrTiO_3$ (STO),[2] or, more recently, between $LaGaO_3$ and $SrTiO_3$,[3] with surprising properties such as bistable conductivity, magnetic order, and tunable superconductivity.[4–6] The design of nanoelectronic circuits based on these effects demonstrates a high application potential.[7] However, in spite of intense research efforts, key properties of the 2DEL, such as the microscopic mechanisms driving it and the distribution of charges around the interface, are still controversially discussed. Presently, the emergence of the 2DEL at the LAO/STO interface is ascribed to the electrostatic instability arising from the polar discontinuity at the interface. In the ideal case, the resulting "polar catastrophe"[8] is avoided by the transfer of 1/2 electron per surface unit cell to the interface. This promotes the formation of the 2DEL when $n \geqslant 4$ monolayers of LAO are deposited on the STO. The compelling intuition behind this model is somewhat diminished by the observation that the carrier density expected at the interface is an order of magnitude larger than the density observed in Hall measurements,[4] an issue termed the "missing charge problem."[9] Another highly controversial issue is the width of the 2DEL: propositions range from band-bending scenarios reminiscent of semiconductors[10] to confinement in a single monolayer.[11] Prevalence is toward the latter case but here the experimental resolution (at best a few nm) poses a limit to a reliable estimate.

Here we show that, according to optical second harmonic generation (SHG) spectroscopy, the formation of the 2DEL involves three processes. First, an orbital reconstruction of an interface-related $Ti^{4+}(3d)$ state occurs in the STO monolayer next to the LAO in the course of electrostatic breakdown[12] at $n = 3$, successive to precursors at $n < 3$. Second, the polarization discontinuity polarizes the STO across several monolayers adjacent to the interface, presumably by displacing the Ti^{4+} ions. At this stage, the LAO/STO system remains fully insulating, presumably because all the charge carriers injected into the interface region are trapped. Third, the 2DEL emerges as a disjunct process upon proceeding from $n = 3$ to $n = 4$. This scenario offers a possible explanation for the notorious missing charge problem:[9] with respect to the change of orbital and electronic structure at the interface, conduction seems to be a subordinate effect initiated by a small fraction of carriers upon further increase of the LAO coverage.

Optical SHG is a powerful noninvasive technique specifically sensitive to interfaces. It is based on the induction of light waves of frequency 2ω by incident waves of frequency ω. The interface sensitivity of the SHG process results from its coupling to the broken inversion symmetry at the interface, while contributions from the centrosymmetric bulk material are suppressed.[13,14] More descriptively, the breaking of inversion symmetry in a condensed-matter system corresponds to a displacement of ionic and electronic charges, and SHG probes the ensuing polarization. In the present case the SHG signal therefore reproduces the entire region affected by the reconstruction at the LAO/STO interface, while the regions that are not affected by the reconstruction remain invisible to the SHG process.

Former single-wavelength experiments were pioneering in revealing a coupling of SHG to the processes at the LAO/STO interface[9] and to distinguish confinement-related contributions

from substrate effects,[15] yet without putting emphasis on locating the spectral and spatial origin of the underlying microscopic processes. Here, by exploiting the spectral degree of freedom, we highlight the distribution of polarization spectrally (the electronic state involved in the LAO/STO reconstruction) and spatially (the distribution of the reconstruction around the interface). A detailed derivation of the contributions to the net SHG signal is given in the Appendix.

II. EXPERIMENT

Two sets of samples grown in Naples and Augsburg were investigated under ambient conditions. A slightly different growth procedure[9] was applied. Since all the following observations are reproduced in both sets, the results appear to be robust against growth-induced defects. In both sets, interfacial conduction (sheet conductance $\sigma_S = 10^{-5}$–10^{-4} Ω^{-1} at 300 K) emerges at $n = 4$, while all the $n < 4$ samples show a sheet conductance below the detection limit of 10^{-9} Ω^{-1}. A standard linear-optical characterization was performed by spectroscopic ellipsometry.

In the present SHG spectroscopy experiment (see the Appendix), frequency-tunable laser pulses of 130 fs are generated at 1 kHz by an optical parametric amplifier pumped by a Ti:sapphire amplifier system. Pulses with a typical fluence of 3 to 5 mJ/cm^2 are incident at 45° to the sample surface and focused onto a spot with a diameter of ~ 180 μm. A standard reflection setup was used for measuring the SHG spectra.[16] Between 1.5 and 3.3 eV the SHG yield is small and all spectra are featureless. We will therefore focus on the spectral region from 3.20 eV up to 3.75 eV. The symmetry of the LAO/STO interface is $4mm$ with z as the fourfold axis perpendicular to the interface. According to Ref. 17 this symmetry allows only three independent nonzero contributions to the SHG susceptibility: (i) $\chi_{zxx} = \chi_{zyy}$, (ii) $\chi_{xxz} = \chi_{xzx} = \chi_{yyz} = \chi_{yzy}$, and (iii) χ_{zzz}. The experimental configurations for accessing these components (or linear combinations of them) are listed in Table I.

III. RESULTS AND DISCUSSION

Figure 1 shows the pp, ds, and sp spectra (notation as in Table I) with the LAO coverage n ranging from 0 to 12 monolayers. All SHG spectra display a resonance at 3.6 eV with a width of ≈ 0.1 eV which is followed by a pronounced positive slope extending beyond 3.7 eV. The same features are found in the $n = 0$ sample, i.e., in the bare STO substrate, whereas the single-crystal surface of a bare LAO (001) sample yields a negligibly small SHG signal. This is a first indication that the STO is the only source of the SHG signal.

TABLE I. Nonzero tensor components and polarization configurations for SHG on the LAO/STO interface. According to Ref. 17, three independent SHG tensor components are allowed for the $4mm$ symmetry of the interface: χ_{zxx} and χ_{xxz} are accessed by a single polarization configuration, while χ_{zzz} is included in a linear combination. Polarizations are denoted by p (parallel to the plane of incidence), s (parallel to the sample surface) and d (at 45° between the p and s polarizations).

Polarization configuration		SHG
Ingoing	Outgoing	susceptibility
s	p	$\chi_{zxx} = \chi_{zyy}$
d	s	$\chi_{xxz} = \chi_{xzx} = \chi_{yyz} = \chi_{yzy}$
p	p	$a\chi_{zzz} + a'\chi_{zxx} + a''\chi_{xxz}$

The slope indicates the band edge of the $O^{2-} \rightarrow Ti^{4+}$ charge-transfer excitation which was, for instance, observed by optical absorption measurements.[18] Even though this is associated with a bulk excitation the breaking of inversion symmetry at the interface is required to observe it by SHG. In contrast, the resonance at 3.6 eV is qualitatively new and indicates the possible presence of a state bound to the interface but nonexisting in the bulk. In order to identify this interface-sensitive contribution we first derived the SHG spectrum under the assumption that all orbitals stay "bulk-like" even at the interface.[19] For this purpose, we fitted the spectra by the expression $I(2\omega) = |\sum_k A_k/(2\omega - \omega_k + i\gamma_k)|^2$, where A_k are fit parameters and ω_k and γ_k are the interband resonances and their widths, respectively, as measured directly by ellipsometry. A best-fit curve is shown in Fig. 2, exemplarily choosing the $n = 6$ sample. The slope extending beyond 3.7 eV correctly reproduces the direct cross-band-gap transition edge of the STO, i.e., the electronic transitions between the valence O^{2-} and the Ti^{4+} conduction band.[20] This clearly confirms that the STO is the only source of the SHG signal. The simulation does not reveal any indication of the resonance at 3.6 eV. Since this resonance is present in the $n = 0$ sample as well, it must be ascribed to a polar surface-bound electronic state in the vicinity of the $O^{2-} \rightarrow Ti^{4+}$ transition.

At $n = 3$, a steep gradient of the SHG yield in the spectral range of the $Ti^{4+} \rightarrow O^{2-}$ transition reveals a major change in the polarization of either the $Ti^{4+}(3d[t_{2g}])$ or the $O^{2-}(2p)$ orbitals. Since in STO the Ti^{4+} ions are known to be easily displaceable[21] and density-functional calculations predict a pronounced shift of Ti^{4+} ions near the boundary,[22] it is straightforward to ascribe the increase of the polar asymmetry to a polarization change of the Ti^{4+} orbitals. Note that the increment at $n = 3$ cannot be due to LaO-TiO_2 ionic intermixing effects, because these are already present at $n < 3$. Reproducible anomalies for $n = 1$ (sp) and $n = 2$ (pp) already indicate minor anisotropic modifications of the interface structure, but aside from these precursors the main transition clearly occurs at $n = 3$. In contrast to the conductivity measurements, the SHG spectra reveal only a minor difference between the samples with $n = 3+$ (insulating) and $n = 4$ (conducting), an issue that will be discussed later on. Note that although the discontinuity of the SHG signal at $n = 3$ has been already reported,[9,15] it is the spectroscopic information gained here that allows us to associate this phenomenon to major polarization changes in the $Ti^{4+}(3d[t_{2g}])$ state.

The spectral dependence of the SHG signal in Fig. 1 is quite intriguing. The uniform enhancement of the SHG spectrum upon increasing the number of LAO monolayers from two to three shows that the polarization of *rather different* spectral transitions are enhanced by the interface reconstruction: that of the *bulk-like* state represented by the 3.7 eV slope and that of the *surface* state represented by the 3.6 eV peak. In particular, (i) the surface state is not the only state to be modified by the interface reconstruction; (ii) none of the

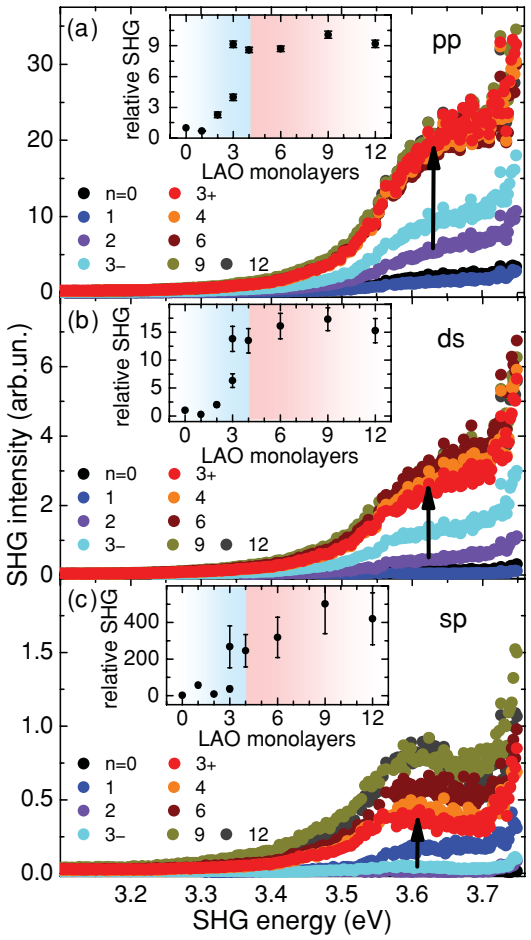

FIG. 1. (Color online) SHG spectra of the LAO/STO interface for varying thickness of the LAO films (counted in the number of monolayers n) and different polarization combinations (notation as in Table I). The same relative scale for the SHG intensity is used in all plots. The SHG energy is $2\hbar\omega$ with ω as frequency of the incoming light. Vertical arrows indicate the reconstruction occurring at the critical thickness $n = 3$, where a pronounced sample-to-sample spread in the SHG yield is observed, with the extremes being labeled 3+ and 3−. The insets show the relative change of the SHG yield compared to the value at $n = 0$, integrated on the whole spectrum.

electronic orbitals probed here are shifted in energy in the course of the transition. We conclude that the surface state and the bulk-like state merely *respond* to polarizing effects generated *elsewhere*. Here "elsewhere" refers to the site of the *primary* orbital reconstruction that, apparently, has not been located yet.

In order to elucidate this issue, we focus our attention on the χ_{zzz} susceptibility component. With three z polarized light waves involved, it is expected to display a particularly enhanced interface sensitivity because of the structural and, thus, polarization discontinuity along z.[23] According to Table I, the component cannot be measured directly but has to be extracted from the *pp* spectra. For this purpose, two fundamental parameters have to been determined: the spectral dependance of the coefficient a', a'', and a''' [see Appendix, Eqs. (A5) and (A6)] and the relative phases between the components χ_{zzz}, χ_{zxx}, and χ_{xxz}. On the basis of Eq. (A4) the former can be directly derived from measuring the index of refraction of STO.

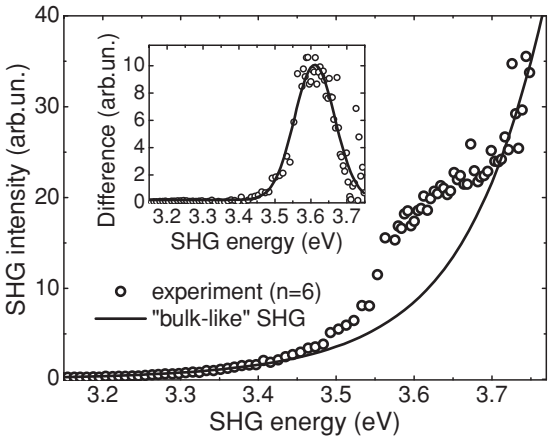

FIG. 2. Bulk and surface contributions to the SHG spectrum. Data points: Exemplary SHG spectrum at $n = 6$ for the *pp* configuration. Line: theoretical bulk-like SHG signal derived from ellipsometry measurements (see text). Inset: The difference between data and fit reveals the surface-related state at 3.6 eV. The line is a guide to the eye.

The relative phase between the three components χ_{zzz}, χ_{zxx}, and χ_{xxz} can be acquired by polarization-dependent SHG:[24] for three output polarizations (p, s, d) the SHG signal is measured at several wavelengths as a function of the angle α denoting the polarization of the incident light. Then, the data can be fitted on the basis of Eq. (A7). Exemplary SHG polarization measurements are shown in Fig. 3(b). The separation of χ_{zxx}, χ_{xxz}, and χ_{zzz} leads to the data sets shown in Fig. 4. Note that the magnitude of χ_{zzz} is about a factor of 10 larger than the contributions from χ_{zxx} and χ_{xxz}.

In fact, striking differences are found between the $\chi_{zxx,xxz}$ spectra and the χ_{zzz} spectra in Fig. 4. First of all, χ_{zzz} couples to the surface-induced state at 3.6 eV, but *not* to the cross-band-gap transition edge beyond 3.7 eV. Most remarkably, a comparison between $n \geqslant 3$ and $n < 3$ samples in Fig. 4 shows that, while the amplitude of χ_{zzz} is roughly independent of n, its spectral weight is strongly redistributed across the transition. In particular, beyond the transition the spectral weight above 3.7 eV is strongly suppressed in favor of an increase of the spectral weight around 3.6 eV. The independence of the SHG yield is most likely caused by the symmetry breaking at the surface which dominates the χ_{zzz} amplitude irrespective of the explicit value of n. The spectral changes suggest a band splitting due to an orbital reconstruction within the Ti^{4+} surface state. Note that the spectral weight appears to be downshifted by about 0.1 eV. Theoretical calculations are in excellent agreement with this scenario: according to Ref. 25, the spectral redistribution may be caused by a crystal-field splitting of the order of 0.1 eV due to population of the d_{xy} orbital. This is predicted to occur at $n \approx 3.5$ which matches $n = 3$ in our data.

Most importantly, the splitting is calculated to occur only at the *very first* STO interface monolayer.[25] This agrees very well with the following orders-of-magnitude estimate: as mentioned, the χ_{zzz} component involving three light waves polarized perpendicular to the LAO/STO interface is interface-dominated, therefore revealing the primary orbital reconstruction originating at the interface. The χ_{xxz} and χ_{zxx} components involve tangential light waves, too, and are

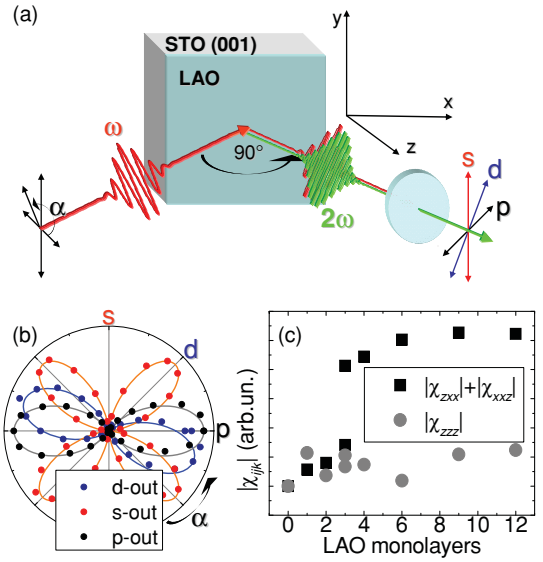

FIG. 3. (Color online) (a) Experimental scheme and polarization geometry. (b) Normalized SHG signal in dependence of the polarization α of the incident fundamental light for fixed output polarizations (s red, p black, d blue) of the SHG light. (c) The $|\chi_{zzz}|$ and $|\chi_{zxx}|+|\chi_{xxz}|$ moduli vs n at 3.6 eV. Each data set has been normalized to the $n=0$ values for a better comparison, since $|\chi_{zzz}|$ is larger by a factor 10. The data points were derived from polarization-dependent SHG data as in (b). Note that (c) shows susceptibility data ($\propto \chi$) at a single photon energy (the peak of the surface state) while Fig. 1 shows spectrally integrated intensity data ($\propto \chi^2$). In the former the transition centered at $n=3$ is more pronounced.

therefore not exclusively interface-dominated. Instead, they reveal the polarization of the entire region affected by the interface reconstruction: the polarization associated with the *primary* orbital reconstruction bound to the interface but also the polarization associated with the ionic shifts away from the interface that are *induced* by the orbital reconstruction. However, the χ_{xxz} and χ_{zxx} spectra show none of the energy splitting that characterizes the orbital reconstruction. Apparently the contribution of the primary orbital reconstruction to the SHG yield in χ_{xxz} and χ_{zxx} spectra is so small that the energy splitting is obscured by the SHG contribution from the ionic shifts whose energy does not change with n. Assuming that the orbital and the ionic contributions to the polarization couple to the SHG with a similar efficiency, we can thus conclude that the contribution to SHG from the orbital polarization is at least one order of magnitude lower than that of the ionic polarization. From Ref. 15 we know that the SHG signal associated with the ionic displacements stems from about eight monolayers of STO next to the LAO/STO interface. Consequently, the SHG signal related to the orbital reconstruction is found to be associated mostly with a single layer.

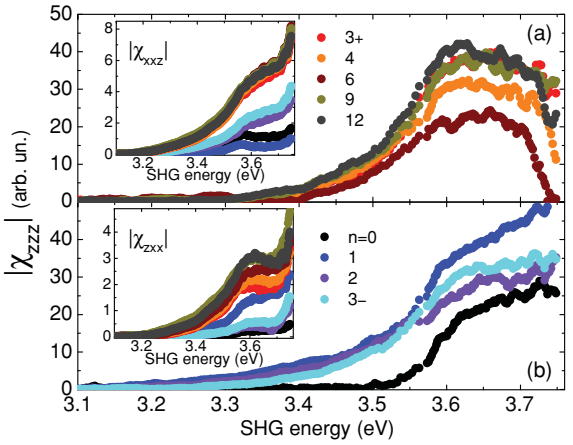

FIG. 4. (Color online) Analysis of the pp contribution to SHG. Spectral dependence of $|\chi_{zzz}|$ for samples with $n \geqslant 3$ (upper panel) and $n \leqslant 3$ (lower panel). For comparison, the upper and lower inset shows the $|\chi_{xxz}|$ and $|\chi_{zxx}|$ spectra, respectively.

We stress that in spite of the semiquantitative quality of this estimate, we clearly see that the region affected by the LAO/STO interface reorganization is much wider than the region where the actual orbital reconstruction occurs. Our estimate suggests that the orbital reconstruction affects predominantly the first STO monolayers next to the LAO/STO interface. In addition, the reconstruction polarizes the STO across several subsequent monolayers. The scenario is supported by the calculations in Ref. 25 and does not contradict previous SHG experiments[9,15] or a variety of other experimental works.[11,26–28]

An issue that remains to be clarified is the separation of the orbital reconstruction at $n=3$ from the emergence of the 2DEL at $n=4$. Indications for a precursor behavior at $n<4$ have been found in a variety of experiments,[9,15,29,30] including the present one. The most pronounced discontinuity is observed when the SHG yield jumps by a factor of 4–30 upon going from $n=2$ to $n=3+$ (Fig. 1) while the change upon going from $n=3+$ (insulating) to $n=4$ (conducting) is minor.

Apparently, the charge carriers are still localized at the LAO/STO interface when the major carrier-induced orbital reconstruction has occurred. We can only speculate about the trapping mechanism. It is known that the d_{xy} orbitals are prone to disorder-induced localization[22] so that local disorder may trap the carriers. Alternatively, the LAO may stabilize a self-trapped polaron, which is at least transiently present in STO exposed to UV illumination.[31] It is remarkable that in terms of the SHG data the emergence of conduction is clearly separated from the orbital reconstruction. A variety of mechanisms may contribute to this: (i) SHG may be less sensitive to mobile than to localized carriers; (ii) application of the fourth LAO monolayer may free some of the carriers trapped at $n=3$, so that the total number of carriers at the interface (and the associated SHG yield) may not change; (iii) the number of carriers contributing to conduction may be much smaller than the number of trapped carriers contributing to the orbital reconstruction. This latter point would also give a simple solution to the aforementioned missing charge problem.[4]

IV. CONCLUSIONS

In summary, optical SHG spectroscopy reveals that the generation of the 2DEL at the LAO/STO interface is rooted

in a reconstruction of the $Ti^{4+}(3d)$ orbitals centered around $n = 3$ monolayers coverage. The reconstruction manifests as a spectral redistribution of a previously unknown Ti^{4+}-related surface state. According to an orders-of-magnitude estimate, it predominantly affects a single STO monolayer next to the interface. It is accompanied by a buildup of polarization in several monolayers around the interface and presumably caused by small displacements of the Ti^{4+} ions. The carriers involved in the orbital reconstruction are trapped. The onset of conduction occurs separately at $n = 4$. It involves a minority of carriers and leads to the emergence of a 2DEL with only minor changes of the electronic states involved.

Our observations have a variety of consequences for technological applications involving the 2DEL. First, the pronounced confinement places the oxide interfaces discussed here in great distance to semiconductors, where spatially extended band-bending leads to interface conduction. Second, we propose a simple explanation to the missing charge problem, which may help to find strategies for increasing the interfacial carrier concentration. Third, hysteresis and bistability effects in the conduction that are the basis for the design of electronic nanocircuits henceforth need to be related to the control of the carrier trapping (rather than electric fields) at the interface. Modifications of the population density at the interface, e.g., by resonant optical pumping of the surface-bound state observed in the STO, may be used for reversible ultrafast conductivity control.

ACKNOWLEDGMENTS

The research leading to these results has received funding from DFG (SPP 1133, TRR 80), the FP7 2007-2013 under Grant Agreement No. 264098 - MAMA, the EU (OxIdes), and by Ministero dell'Istruzione, dell'Università e della Ricerca under Grant Agreement PRIN 2008 - 2DEG FOXI.

APPENDIX : SHG theory

The constitutive equation of the SHG process is

$$P_i(2\omega) = \varepsilon_0 \chi_{ijk} E_j(\omega) E_k(\omega), \tag{A1}$$

where $\mathbf{E}(\omega)$ is the electric field of the incident wave, $\mathbf{P}(2\omega)$ is the induced nonlinear optical polarization, and $\hat{\chi}$ is the SHG susceptibility tensor. The measured quantity in SHG spectroscopy is the SHG intensity $I_{\mathrm{SHG}}(2\omega) \propto |\vec{P}(2\omega)|^2$. I_{SHG} is proportional to the square of the reflected SHG electric field: $I_{\mathrm{SHG}} \propto |E_{\mathrm{SHG}}|^2$. The latter can, in turn, be written as a function of the electric field incident onto the sample:

$$E_{\mathrm{SHG}} = \frac{i\omega E_0^2}{\epsilon_0 c \cos\beta} \chi_{\mathrm{eff}}, \tag{A2}$$

with E_0 as the electric-field amplitude outside the sample, β as the angle of incidence, and χ_{eff} defined as follows:

$$\chi_{\mathrm{eff}} = e_i^{\mathrm{out}} L_{ii}^{\mathrm{out}} \chi_{ijk} L_{jj}^{\mathrm{in}} L_{kk}^{\mathrm{in}} e_j^{\mathrm{in}} e_k^{\mathrm{in}}. \tag{A3}$$

Here, $\mathbf{e}^{\mathrm{in,out}}$ are the unit vectors of the optical polarization in air for the incident fundamental and the emitted SHG wave, and $\mathbf{L}^{\mathrm{in,out}}$ are the corresponding Fresnel transformations.

Now we assume that both input and output waves are linearly polarized, with an angle α with respect to the incidence plane (xy). It is useful to denote the polarizations with the following notation: p – parallel to the incidence plane ($\alpha = 0$), s – parallel to the sample surface plane ($\alpha = \pi/2$), and d – at 45° between p and s ($\alpha = \pi/4$).

The three nonzero components of the diagonal tensor $\mathbf{L}$ are given by[32]

$$\begin{aligned} L_{xx}(\omega) &= \frac{2n_1(\omega)\cos\beta'}{n_2(\omega)\cos\beta + n_1(\omega)\cos\beta'}, \\ L_{yy}(\omega) &= \frac{2n_1(\omega)\cos\beta}{n_1(\omega)\cos\beta + n_2(\omega)\cos\beta'}, \\ L_{zz}(\omega) &= \frac{2n_2(\omega)\cos\beta}{n_2(\omega)\cos\beta + n_1(\omega)\cos\beta'} \left(\frac{n_1(\omega)}{n'(\omega)}\right)^2, \end{aligned} \tag{A4}$$

where β' is the angle of incidence inside the material, n_1 the refractive index of air, and n_2 the refractive index of bulk STO as measured, for instance, by ellipsometry.[33] Note that n' is the refractive index of the SHG-active interfacial layer. For a quantitative analysis of the interface properties (such as a calculation of an absolute value of the polarization asymmetry at the LAO/STO interface) it is essential to distinguish n' from the bulk values n_1 and n_2.[32] However, the scope of Sec. III is a basic orders-of-magnitude model for the orbital and polarization states at the LAO/STO interface. In this case, the choice of $n' = n_1$ or $n' = n_2$ is an established approximation.[34] Here we treat the interface as being embedded in STO and therefore set $n' = n_2 \equiv n$.

Because of the perovskite structure of the bulk crystal, the LAO/STO interface has the symmetry $4mm$. According to Ref. 17 three independent tensor components are allowed for $\hat{\chi}$ as listed in Table I. Note that these tensor components are in general complex numbers with phase and modulus.

Two of them, χ_{zxx} and χ_{xxz}, can be singled out by an appropriate choice of the input and output polarizations, while χ_{zzz} is always mixed with the other two. In particular, it is useful to write χ_{eff} for the s-input p-output (sp) and the d-input s-output (ds) polarization combinations, which contain χ_{zxx} and χ_{xxz}, respectively, and for the p-input p-output (pp) combination, which contains all three components:

$$\begin{aligned} \chi_{sp}^{\mathrm{eff}} &= \chi_{zxx} L_{zz}^{\mathrm{out}} \left(L_{yy}^{\mathrm{in}}\right)^2 \sin\beta, \\ \chi_{ds}^{\mathrm{eff}} &= \chi_{xxz} L_{yy}^{\mathrm{out}} L_{yy}^{\mathrm{in}} L_{zz}^{\mathrm{in}} \sin\beta, \\ \chi_{pp}^{\mathrm{eff}} &= a\chi_{zzz} + a'\chi_{zxx} + a''\chi_{xxz}, \end{aligned} \tag{A5}$$

and

$$\begin{aligned} a &= L_{zz}^{\mathrm{out}} \left(L_{zz}^{\mathrm{in}}\right)^2 \sin^3\beta, \\ a' &= L_{zz}^{\mathrm{out}} \left(L_{xx}^{\mathrm{in}}\right)^2 \sin\beta\cos^2\beta, \\ a'' &= -2L_{xx}^{\mathrm{out}} L_{zz}^{\mathrm{in}} L_{xx}^{\mathrm{in}} \sin\beta\cos^2\beta. \end{aligned} \tag{A6}$$

Using the measured values for the STO refractive index of 2.33 for the fundamental light (photon energy 1.8 eV) and 2.99 for the SHG (photon energy 3.6 eV) one can calculate that a is 20 times smaller than a'' for $\beta = 45°$ and still 10 times smaller for $\beta = 80°$. This means that it is not possible to separate χ_{zzz} experimentally from the much larger components χ_{zxx} and χ_{xxz}. Instead, χ_{zzz} has to be extracted *a posteriori* from the

SHG data. For this purpose, two fundamental parameters have to been determined: the spectral dependance of the coefficient in Eq. (A5) and the relative phases between the three components. The former can be directly inferred from the index of refraction n through Eq. (A4), while the latter task can be achieved by polarization-dependent SHG measurements: The SHG signal is measured for several wavelengths as a function of the incoming polarization angle α, for three fixed output polarizations, namely, p, s, and d. The data can be then fitted exploiting the following relationship:

$$\begin{aligned} \alpha - \text{in}, s - \text{out SHG} &: \chi_{\alpha s}^{\text{eff}} = \chi_{xxz} L_{yy}^{\text{out}} L_{yy}^{\text{in}} L_{zz}^{\text{in}} \sin\beta \sin 2\alpha, \\ \alpha - \text{in}, p - \text{out SHG} &: \chi_{\alpha p}^{\text{eff}} = \chi_{sp}^{\text{eff}} \sin^2\alpha + \chi_{pp}^{\text{eff}} \cos^2\alpha, \\ \alpha - \text{in}, d - \text{out SHG} &: \chi_{\alpha d}^{\text{eff}} = \frac{\chi_{\alpha s}^{\text{eff}} + \chi_{\alpha p}^{\text{eff}}}{\sqrt{2}}. \end{aligned} \quad \text{(A7)}$$

*paparo@na.infn.it

[1] R. Ramesh and D. G. Schlom, MRS Bull. **33**, 1006 (2008).

[2] A. Ohtomo and H. Y. Hwang, Nature (London) **427**, 423 (2004).

[3] P. Perna, D. Maccariello, M. Radovic, U. S. di Uccio, I. Pallecchi, M. Codda, D. Marre, C. Cantoni, J. Gazquez, M. Varela, S. J. Pennycook, and F. M. Granozio, Appl. Phys. Lett. **97**, 152111 (2010).

[4] S. Thiel, G. Hammerl, A. Schmehl, C. W. Schneider, and J. Mannhart, Science **313**, 1942 (2006).

[5] A. D. Caviglia, S. Gariglio, N. Reyren, D. Jaccard, T. Schneider, M. Gabay, S. Thiel, G. Hammerl, J. Mannhart, and J.-M. Triscone, Nature (London) **456**, 624 (2008).

[6] A. Brinkman, M. Huijben, M. Van Zalk, J. Huijben, U. Zeitler, J. C. Maan, W. G. Van der Wiel, G. Rijnders, D. H. A. Blank, and H. Hilgenkamp, Nat. Mat. **6**, 493 (2007).

[7] C. Cen, S. Thiel, J. Mannhart, and J. Levy, Science **323**, 1026 (2009).

[8] H. Y. Hwang, Science **313**, 1895 (2006).

[9] A. Savoia, D. Paparo, P. Perna, Z. Ristic, M. Salluzzo, F. Miletto Granozio, U. Scotti di Uccio, C. Richter, S. Thiel, J. Mannhart, and L. Marrucci, Phys. Rev. B **80**, 075110 (2009).

[10] K. Yoshimatsu, R. Yasuhara, H. Kumigashira, and M. Oshima, Phys. Rev. Lett. **101**, 026802 (2008).

[11] M. Sing, G. Berner, K. Goss, A. Müller, A. Ruff, A. Wetscherek, S. Thiel, J. Mannhart, S. A. Pauli, C. W. Schneider, P. R. Willmott, M. Gorgoi, F. Schaefers, and R. Claessen, Phys. Rev. Lett. **102**, 176805 (2009).

[12] N. Nakagawa, H. Y. Hwang, and D. A. Muller, Nat. Mat. **5**, 204 (2006).

[13] Y. R. Shen, Surf. Sci. **299/300**, 551 (1994).

[14] De Sheng Zheng, Yuan Wang, An-An Liu, and Hong-Fei Wang, Int. Rev. Phys. Chem. **27**, 629 (2008).

[15] N. Ogawa, K. Miyano, M. Hosoda, T. Higuchi, C. Bell, Y. Hikita, and H. Y. Hwang, Phys. Rev. B **80**, 081106(R) (2009).

[16] M. Fiebig, N. P. Duong, T. Satoh, B. B. Van Aken, K. Miyano, Y. Tomioka, and Y. Tokura, J. Phys. D **41**, 164005 (2008).

[17] R. R. Birss, *Symmetry and Magnetism* (North Holland, Amsterdam, 1966).

[18] D. Goldschmidt and H. L. Tuller, Phys. Rev. B **35**, 4360 (1987).

[19] G. Erley, R. Butz, and W. Daum, Phys. Rev. B **59**, 2915 (1999).

[20] K. Van Benthem, C. Elsässer, and R. H. French, J. Appl. Phys. **90**, 6156-6164 (2001).

[21] A. A. Sirenko, C. Bernhard, A. Golnik, A. M. Clark, J. H. Hao, W. D. Si, and X. X. Xi, Nature (London) **404**, 373 (2000).

[22] Z. S. Popović, S. Satpathy, and R. M. Martin, Phys. Rev. Lett. **101**, 256801 (2008).

[23] A. V. Petukhov and A. Liebsch, Surf. Sci. **334**, 195 (1995).

[24] Y. Tanabe, M. Muto, M. Fiebig, and E. Hanamura, Phys. Rev. B **58**, 8654 (1998).

[25] J. Lee and A. A. Demkov, Phys. Rev. B **78**, 193104 (2008).

[26] M. Basletic, J.-L. Maurice, C. Carretero, G. Herranz, O. Copie, M. Bibes, E. Jacquet, K. Bouzehouane, S. Fusil, and A. Barthelemy, Nat. Mat. **7**, 621 (2008).

[27] T. Fix, F. Schoofs, J. L. MacManus-Driscoll, and M. G. Blamire, Phys. Rev. Lett. **103**, 166802 (2009).

[28] I. Pallecchi, M. Codda, E. Galleani dAgliano, D. Marré, A. D. Caviglia, N. Reyren, S. Gariglio, and J.-M. Triscone, Phys. Rev. B **81**, 085414 (2010).

[29] M. Salluzzo, J. C. Cezar, N. B. Brookes, V. Bisogni, G. M. De Luca, C. Richter, S. Thiel, J. Mannhart, M. Huijben, A. Brinkman, G. Rijnders, and G. Ghiringhelli, Phys. Rev. Lett. **102**, 166804 (2009).

[30] M. Huijben, G. Rijnders, D. H. A. Blank, S. Bals, S. Van Aert, J. Verbeeck, G. Van Tandeloo, A. Brinkman, and H. Hilgenkamp, Nat. Mater. **5**, 356 (2006).

[31] K. Nasu, Phys. Rev. B **67**, 174111 (2003).

[32] X. Zhuang, P. B. Miranda, D. Kim, and Y. R. Shen, Phys. Rev. B **59**, 12632 (1999).

[33] R. M. A. Azzam and N. M. Bashara, *Ellipsometry and Polarized Light* (North Holland, Amsterdam, 1977).

[34] T. G. Zang, C. H. Zhang, and G. K. Wong, J. Opt. Soc. Am. B **7**, 902 (1990).